CHINESE OPTICS LETTERS

Vol. 21, No. 10 | October 2023

Integrated fluorescence excitation, collection, and filtering on a GaN waveguide chip

Jiahui Zhang (张家晖)[1,2,†], Feng Xu (徐 峰)[1,2,†], Ran An (安 然)[1,2], Lin Wang (王 琳)[1,2], Min Jiang (江 敏)[3], Guanghui Wang (王光辉)[1,2*], and Yanqing Lu (陆延青)[1**]

[1] College of Engineering and Applied Sciences, Nanjing University, Nanjing 210093, China

[2] Key Laboratory of Intelligent Optical Sensing and Integration of the Ministry of Education, Nanjing University, Nanjing 210009, China

[3] College of Science, Wuxi University, Wuxi 214411, China

*Corresponding author: wangguanghui@nju.edu.cn

**Corresponding author: yqlu@nju.edu.cn

Received April 27, 2023 | Accepted May 25, 2023 | Posted Online October 10, 2023

Fluorescence detection is widely used in biology and medicine, while the realization of on-chip fluorescence detection is vital for the portable and point-of-care test (POCT) application. In this Letter, we propose an efficient fluorescence excitation and collection system using an integrated GaN chip consisting of a slot waveguide and a one-dimensional photonic crystal (1D PC) waveguide. The slot waveguide is used to confine the excitation light for intense light–sample interaction, and the one-trip collection efficiency at the end of slot waveguide is up to 14.65%. More interestingly, due to the introduction of the 1D PC waveguide, the fluorescence signal is directly filtered out, and the excitation light is reflected to the slot waveguide for multiple excitations. Its transmittances for the designed exciting wavelength of 520 nm and the fluorescent wavelength of 612 nm are 0.2% and 85.4%, respectively. Finally, based on numerical analysis, the total fluorescence collection efficiency in our system amounts to 15.93%. It is the first time, to our knowledge, that the concept of an all-in-one-chip fluorescence detection system has been proposed, which paves the way for on-chip fluorescence excitation and collection, and may find potential applications of miniaturized and portable devices for biomedical fluorescence detection.

Keywords: fluorescence; slot waveguide; photonic crystal; on-chip.

DOI: 10.3788/COL202321.101203

1. Introduction

Fluorescence has been found as a powerful detection method in biotechnology[1], medicine[2], and related areas[3]. Excitation, collection, and filtering are the key technologies for fluorescence detection. In the traditional cases, the biomedical fluorescence detection is achieved in a bulky desktop microscope, with an objective lens for light focusing and an optical filter set for signal filtering. Nowadays, the rapid development of lab-on-a-chip technologies[4–6] and photonic waveguide integration processes[7–11] provide necessary conditions for the on-chip integration of fluorescence detection. It is expected that fluorescence detection not only should be integrated on a single chip for miniaturization and portability, but also should support higher fluorescence collection efficiency to improve fluorescence detection sensitivity.

Over the years, various waveguide structures that improve fluorescence excitation and coupling efficiency have been demonstrated. Ozhikandathil *et al.* have proposed an evanescent cascaded waveguide coupler for fluorescence detection, and the detection limit of recombinant bovine somatotropin (rbST) in milk was 25 ng/mL[12]. Abdul-Hadi *et al.* have utilized a novel SU-8 waveguide-on-quartz substrate for evanescent fluorescence spectroscopy, with collection efficiency of 10.3% at the top of the waveguide[13]. Since most of the energy is confined inside the waveguide, the mode distribution of the evanescent wave around the waveguide is very weak, and the fluorescence excitation efficiency is limited. Therefore, the challenge is the small overlap of fluorescent sample and waveguide mode, which also limits its fluorescence coupling efficiency[14]. In addition, in most of previously reported works, the separation of excitation and fluorescence wavelength still requires the help of external optical filter in a microscopy system. We also need to look for an all-in-one-chip solution for a fluorescence detection system with strong light–matter interaction and on-chip filtering.

The slot waveguide structure has been widely used to confine the light in the gap filled with samples, which enables strong light–sample interaction[15,16]. Therefore, the fluorescence can be excited and collected more effectively in the slot[14,17]. On

the other hand, one-dimensional photonic crystal 1D PC waveguides could be used as on-chip filters[18,19], which possess smaller footprints and smooth geometry for on-chip integration. Therefore, these configurations pave the way for more efficient fluorescence excitation, collection, and even on-chip filtering to realize an integrated on-chip device.

In this Letter, we propose an on-chip fluorescence excitation, efficient collection, and fluorescence filtering system by using the integrated GaN chip. The system consists of a slot waveguide, a 1D PC waveguide, and two Y-split waveguides. Numerical methods are used to analyze light confinement in the slot waveguide for intense light–sample interaction. Then, the 1D PC waveguide is used as an on-chip photonic filter, which allows the fluorescence signal to pass and the excitation light to be reflected back to the slot waveguide for multiple excitations. Therefore, the total efficiency of the fluorescence detection system could be optimized and can be embedded in a microfluidic chip for the scenario of all-in-one-chip applications.

2. Design of OGFCS

The concept of an integrated fluorescence detection chip is shown in Fig. 1. For the portable and rapid purposes in environmental or water quality testing, biomedical detection, and other fields, the system is placed in a cartridge (black) containing windows for a light source and detector. For fluorescence collection, the cartridge also comprises a microfluidic chamber with an inlet and an outlet for liquid analyte solution. This also prevents the tested sample from affecting the 1D PC. When the solution containing fluorescent material enters the chamber from the inlet, the fluorescent material will fill the slot of waveguide. The excitation light is coupled to the complete system by grating coupler (GC) arrays and then launched into the slot mode through the Y-split waveguide in an on-chip GaN fluorescence detection system (OGFCS). The fluorescence is excited by the excitation light and coupled into the slot waveguide. By the second Y-split waveguide, both the fluorescence and excitation light will be converted from the slot mode to the fundamental mode (TE). Finally, the fluorescence can pass through the 1D PC waveguide while excitation light will be reflected for multiple excitations. When fluorescence reaches the end of the system, it will enter the fluorescence analysis instrument coupled by GC arrays for rapid analysis. Compared with traditional technology, our chip is integrated, portable, and rapid for fluorescence collection and analysis.

To demonstrate the viability of the chip concept shown in Fig. 1, the design of OGFCS is shown in Fig. 2(a). Because only a quasi-TE-polarized mode can be well converted to the slot mode[12], a quasi-TE-polarized excitation light with the wavelength of 520 nm is supposed to excite fluorescent material (e.g., flazo orange), whose fluorescent wavelength is centered at 612 nm. Therefore, the system places the slot waveguide area in the reaction chamber, immersing it in a water environment containing fluorescent material ($n = 1.333$). For low-loss transmitting in visible light range, sapphire and GaN are suitable waveguide materials. The refractive index of GaN is 2.4, while that of sapphire is 1.76, which matches the refractive index of water. Therefore, the GaN waveguide structure is designed on a sapphire substrate, shown in Figs. 2(b) and 2(c). To reduce the fabrication difficulty for the growth of the GaN layer on sapphire substrate due to the severe lattice mismatch between them, an aluminum nitride (AlN) buffer layer is introduced[20]. The thickness of AlN is only a dozen nanometers, with little effect on mode field distribution in the waveguide. Therefore, for simplicity, we can ignore the buffer layer and assume the GaN waveguide is directly located on the sapphire substrate in the simulation[21].

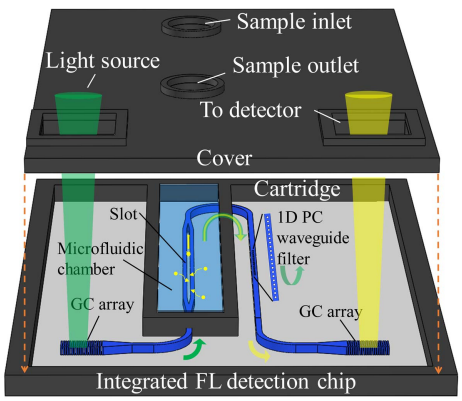

Fig. 1. Concept of an integrated fluorescence detection chip for actual application case.

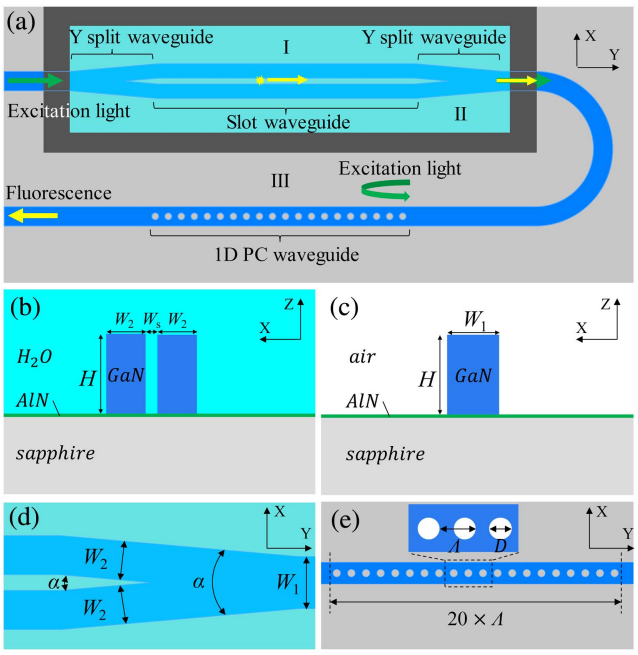

Fig. 2. (a) Schematic diagram of the fluorescence excitation and collection system. Detailed structure of (b) slot waveguide and (c) stripe waveguide; (d) top view of part of the slot waveguide and Y-split waveguide; (e) detailed structure diagram of 1D PC waveguide.

As shown in Fig. 2(a), the height H of all waveguides is 300 nm. In Fig. 2(b), the widths of slot W_s and waveguide W_2 are 60 and 150 nm, respectively. The width of the slot is wide enough for liquid filling[15]. The fluorescence is excited and coupled by a slot mode in the slot waveguide. In Fig. 2(c), the width of the stripe waveguide W_1 is 200 nm so that the fluorescence and excitation light can be transmitted with low loss. Figure 2(d) shows the top view of the Y-split waveguide, which is used for mode conversion (from TE mode to slot mode, or conversely). Both the inner and outer included angles α are optimized to be 10 deg. The 1D PC waveguide consists of 20 periodic holes with the diameter D of 60 nm and the period Λ of 135 nm in one array, as shown in Fig. 2(e). The etch depth of holes is set to be 300 nm. In such a 1D PC structure, the fluorescence light is transmitted, while the excitation light is reflected. Notably, the reflected excitation light will excite the fluorescent material again so that the effect of fluorescence will obviously increase.

3. Simulations and Discussions

Using the finite-difference time-domain (FDTD) method, we calculate the mode pattern of the OGFCS. For the excitation wavelength of 520 nm and different width of W_2, the relation between the normalized power in the slot and the width of slot W_s is shown in Fig. 3(a). The power decreases with the increasing W_s or W_2, due to the mode evolution from slot mode to a couple of fundamental modes. With the decrease of W_2, normalized power will increase gradually while the propagation loss will also increase sharply. Therefore, to keep a balance between strong power in slot and low propagation loss, while considering the fabrication ability, W_2 and W_s are fixed as 150 and 60 nm, respectively, with an acceptable propagation loss of 9.748×10^{-3} dB/μm, which is shown in Fig. 3(b). As shown in Figs. 3(c) and 3(d), the power in the slot for 612 nm wavelength is stronger than that of 520 nm, and the ratio of normalized power in slot are 16.68% and 14.23%, respectively. The figures reveal that the power is high enough for both the exciting wavelength and fluorescent wavelength. Therefore, the fluorescent material will be excited effectively, and fluorescence can be coupled into the stripe waveguide, which will be discussed below.

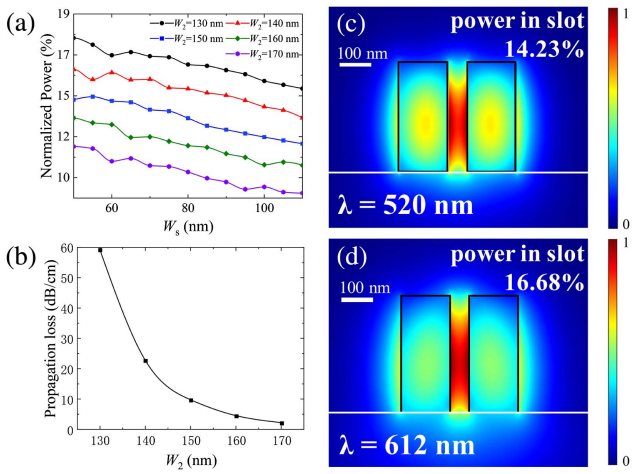

Fig. 3. (a) Graph of the ratio of normalized power in slot versus W_s when W_2 is 130 nm (black dot line), 140 nm (red triangular line), 150 nm (blue square line), 160 nm (green diamond line), and 170 nm (purple hexagonal line) under the wavelength of 520 nm; (b) relationship between propagation loss and W_2; electrical field distributions of the slot waveguide with the wavelengths of (c) 520 nm and (d) 612 nm.

When fluorescence is excited, only part of the energy can be coupled into the slot. Therefore, coupling efficiency will be one of the critical factors in fluorescence collection. To explain the excitation process of fluorescence, a dipole is placed in the slot to simulate the fluorescence exciting, then we calculate the efficiency of fluorescence coupling. Since fluorescence emission has no apparent polarized directivity, and the dipole must operate with a single polarization in our simulations, we appoint the dipoles with x, y, and z directions to calculate the efficiency of fluorescence coupling[14,22,23] separately, as shown in the left part of Fig. 4. When the dipole is x-polarized, as shown in Fig. 4(a), most of the energy will be coupled in the slot of waveguide, just like the slot mode. However, energy emitted from the dipole with y and z directions will couple into the slot with a very low efficiency, as shown in Figs. 4(b) and 4(c).

Figure 4 shows the energy that will couple into the slot effectively only in some specific directions of polarization. However, the electric field distribution cannot quantify the coupling efficiency in either direction. To describe the collecting efficiency of fluorescence in detail, we have calculated the coupling efficiency of polarized dipole luminescence in x, y, and z directions, as shown in Table 1. η_p represents the percentage of energy coupled into the end of the waveguide from total energy emitted by dipole. The position of the detected end is calculated by an overlap integral in simulation. The overlap integral W, which represents the percentage of energy coupled to the waveguide in slot mode, can be calculated by the electric field distribution of the dipole emission and slot mode[23]. Then, the coupling efficiency

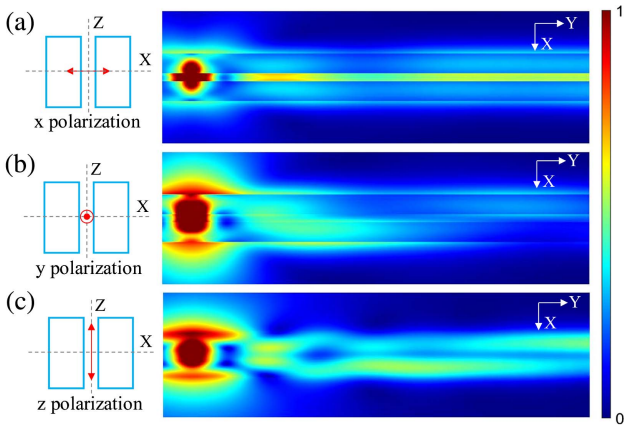

Fig. 4. Propagation of coupled mode in slot when the dipole is polarized in (a) x, (b) y, and (c) z directions.

Table 1. Coupling Efficiency of Fluorescence.

Fig. 4	Polarization Direction	η_p	W	η
(a)	x-polarization	48.52%	0.8856	42.96%
(b)	y-polarization	4.346%	0.2290	0.9951%
(c)	z-polarization	14.30%	0.0001724	0.002465%

η coupled to the slot mode can be represented by multiplying η_p by W.

According to the analysis of coupling efficiency, we find that η of the dipole polarized in the x direction is 42.96%, and most of the light emitted by the dipole is coupled into the slot mode. However, the light emitted by dipoles in the y and z directions will dissipate outside the slot. We have calculated the collection efficiency as 14.65% by averaging η in three directions.

The slot waveguide is not suitable for the 1D PC waveguide to reflect excitation light. So, we designed a slot-stripe converter by the Y-split waveguide, as shown in Fig. 2(a). We have first investigated the relationship between the efficiencies of the slot-stripe converter and the wavelength under different included angles α. As shown in Fig. 5(a), the efficiencies of the slot-stripe converter

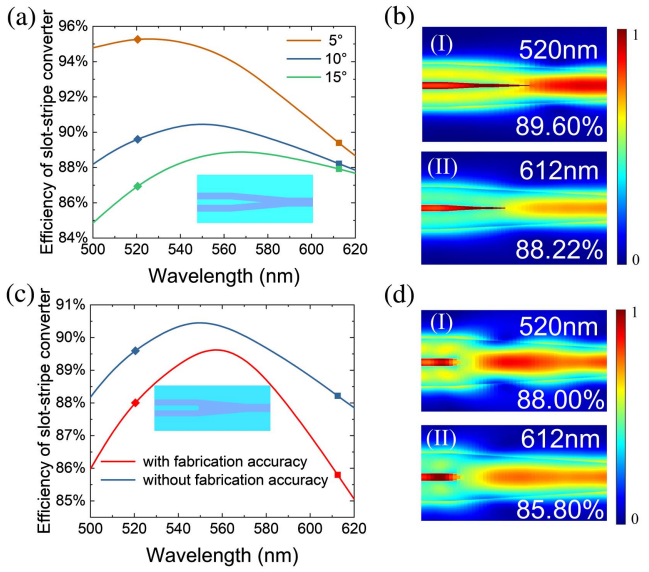

Fig. 5. (a) Relationship between the efficiency of the slot-stripe converter and the wavelength when the included angle α is 5° (orange line), 10° (blue line), and 15° (green line), separately. The diamond and square marks represent exciting and fluorescent wavelengths. (b) Electrical field distributions of the Y-split waveguide with the wavelengths of (I) 520 nm and (II) 612 nm; (c) relationship between the efficiency of the slot-stripe converter and the wavelength under ideal conditions (blue line) and with the consideration of fabrication accuracy (red line) when the included angle α of the Y-split waveguide is 10°; (d) electrical field distributions of the Y-split waveguide with fabrication accuracy for the wavelength of (I) 520 nm and (II) 612 nm.

of both the excitation light and fluorescence are in inverse proportion to α. Considering the balance of efficiency and fabrication ability, we set α as 10°. As shown in Fig. 5(b), it can be found that the conversion efficiency of the excitation light and fluorescence can be up to 89.60% and 88.22%, respectively. The high efficiency proves that such a Y-split waveguide can work as a high-performance converter.

Considering the linewidth limit of electron beam lithography, the included angle α cannot satisfy the design rigorously. Therefore, fabrication accuracy should be considered, and we have smoothed the included angle to a curve due to the circular spot of electron beam to verify the accuracy tolerance when α is 10°. Figure 5(c) shows the comparison of the efficiency of the slot-stripe converter with and without fabrication accuracy taken into account. The efficiency profile of the wavelength almost remains unchanged, and the efficiency will only be reduced by 1.6% and 2.42% for the excitation light and fluorescence. Furthermore, the mode field distributions in Fig. 5(d) show that the mode conversion can also keep stable for both the excitation light and fluorescence. Therefore, fabrication accuracy will almost have no effect on the efficiency of slot-stripe conversion.

According to the previous analysis, both the excitation light and fluorescence are presented in the stripe waveguide. To obtain the fluorescence signal, a 1D PC waveguide is introduced. Compared with the microring resonator, it can achieve a wider fluorescence transmission band and reflect the excitation light for multiple excitations. The number of periodic holes is set as 20, and the depth is 300 nm, which is consistent with the thickness of the waveguide.

Λ and D are set as 135 and 60 nm, and transmittance and reflectivity versus wavelength are shown in Fig. 6(a). The transmittance and reflectivity of the excitation light are 0.2% and 98%, respectively. Therefore, the excitation light will be reflected to the slot waveguide to form a standing wave and excite the fluorescent materials again, as shown in Fig. 6(b). Notably, the powers of one-trip excitation and folded excitation are different because the excitation light is reflected by 1D PC waveguide and has experienced 21.3% propagation loss compared to the pumping light. Furthermore, the ratio in average light intensity of multiple excitations to one-trip excitation has also been calculated as 1.443. Therefore, the fluorescent excitation efficiency will be enhanced 1.443 times because the fluorescence excitation efficiency is proportional to the light intensity.

In addition, the transmittance is greater than 70% when the wavelength is in a wide range of 560 to 620 nm, as shown in Fig. 6(a). Specifically, as in the case discussed in this Letter, the transmittance of fluorescence can even reach 85.4%. We have also simulated the electric field distributions of fluorescence with OGFCS, as shown in Fig. 6(c). Most of the fluorescence passes through the 1D PC waveguide. Noteworthily, because of the great performance of reflectivity and transmittance in the wavelength range of 510 to 530 nm and 560 to 620 nm, the integrated system designed in this Letter can support a wide range of wavelength exciting and collecting, which can provide a wide range of application scenarios.

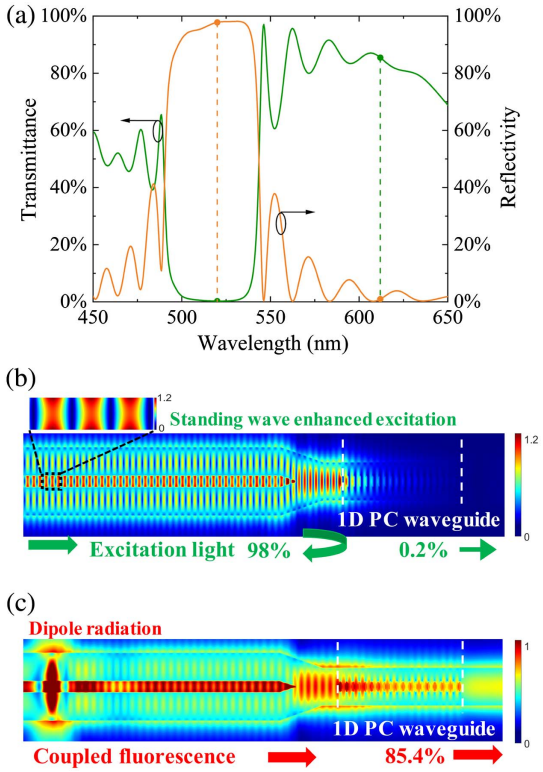

Fig. 6. (a) Function of transmittance (green line) and reflectivity (orange line) with different wavelengths; the orange and green dashed lines represent exciting and fluorescent wavelengths, respectively. Electric field distributions of (b) excitation light and (c) fluorescence with OGFCS.

Now, we can systematically analyze the collection efficiency of fluorescence. First, because the fluorescent excitation efficiency will be enhanced 1.443 times, 21.14% of the fluorescence will be transmitted to the Y-split waveguide. Then, the transmittance of the Y-split waveguide and the 1D PC waveguide with wavelength of 612 nm is 88.22% and 85.4%, respectively, so 15.93% of the excited fluorescence can be finally collected and can be viewed as the collection efficiency of the whole system.

4. Conclusion

In conclusion, we have proposed an all-in-one-chip GaN fluorescence collection system that consists of a slot waveguide, a Y-split waveguide, and a 1D PC waveguide. While the slot waveguide is used to confine the excitation light and enhance light–sample interaction, the one-trip collection efficiency at the end of slot waveguide is up to 14.65%. Very interestingly, the 1D PC waveguide is first introduced in the fluorescence system, which enables us to filter out the fluorescence signal and reflect the excitation light back to the slot waveguide for multiple excitations. When the excitation wavelength is 520 nm, the transmission rate of fluorescence wavelength of 612 nm is 85.4%, while the excitation light is almost completely reflected (transmission rate of 0.2%). Overall, the total fluorescence collection efficiency in our system amounts to 15.93%, which is high for an all-in-one-chip detection system. Our new proposal may promote the development of on-chip integrated fluorescent collection systems and have great prospects for applications in the fields of biomedical sensing, fluorescence detection, etc.

Acknowledgement

This work was supported by the National Natural Science Foundation of China (Nos. 61875083 and 61535005), the Social Development Project of Jiangsu Province (No. BE2019761), and the Key Research and Development Program of Shandong Province (No. 2020CXGC011304).

†These authors contributed equally to this work.

References

1. L. M. Smith, J. Z. Sanders, R. J. Kaiser, P. Hughes, C. Dodd, C. R. Connell, C. Heiner, S. B. Kent, and L. E. Hood, "Fluorescence detection in automated DNA sequence analysis," Nature **321**, 6071 (1986).
2. J. He, C. Li, L. Ding, Y. Huang, X. Yin, J. Zhang, J. Zhang, C. Yao, M. Liang, R. P. Pirraco, J. Chen, Q. Lu, R. Baldridge, Y. Zhang, M. Wu, R. L. Reis, and Y. Wang, "Tumor targeting strategies of smart fluorescent nanoparticles and their applications in cancer diagnosis and treatment," Adv. Mater. **31**, 40 (2019).
3. X. Zhong, X. Wang, L. Sun, and Y. Zhou, "Enhancement of rapid lifetime determination for time-resolved fluorescence imaging in forensic examination," Chin. Opt. Lett. **19**, 041101 (2021).
4. G. Ryu, J. Huang, O. Hofmann, C. A. Walshe, J. Y. Y. Sze, G. D. McClean, A. Mosley, S. J. Rattle, J. C. deMello, A. J. deMello, and D. D. C. Bradley, "Highly sensitive fluorescence detection system for microfluidic lab-on-a-chip," Lab Chip **11**, 1664 (2011).
5. C. Vannahme, S. Klinkhammer, U. Lemmer, and T. Mappes, "Plastic lab-on-a-chip for fluorescence excitation with integrated organic semiconductor lasers," Opt. Express **19**, 8179 (2011).
6. A. Dighe and N. Jokerst, "On-chip fluorescence sensing for fluidics platforms using thin film silicon photodetectors," Biomed. Opt. Express **11**, 5772 (2020).
7. Z. Ding, D. Zhang, G. Wang, M. Tang, Y. Dong, Y. Zhang, H. Ho, and X. Zhang, "An in-line spectrophotometer on a centrifugal microfluidic platform for real-time protein determination and calibration," Lab Chip **16**, 3604 (2016).
8. Z. H. Ren, Y. Chang, Y. Ma, K. Shih, B. Dong, and C. Lee, "Leveraging of MEMS technologies for optical metamaterials applications," Adv. Opt. Mater. **8**, 1900653 (2020).
9. Y. M. Ma, B. W. Dong, and C. K. Lee, "Progress of infrared guided-wave nanophotonic sensors and devices," Nano Converg. **7**, 12 (2020).
10. Z. H. Ren, B. Dong, Q. Qiao, X. Liu, J. Liu, G. Zhou, and C. Lee, "Subwavelength on-chip light focusing with bigradient all-dielectric metamaterials for dense photonic integration," InfoMat **4**, e12264 (2022).
11. X. M. Liu, W. Liu, Z. Ren, Y. Ma, B. Dong, G. Zhou, and C. Lee, "Progress of optomechanical micro/nano sensors: a review," Int. J. Optomechatronics **15**, 120 (2021).
12. J. Ozhikandathil and M. Packirisamy, "Detection of recombinant growth hormone by evanescent cascaded waveguide coupler on silica-on-silicon," J. Biophotonics **6**, 457 (2013).
13. J. Abdul-Hadi, M. A. Gauthier, and M. Packirisamy, "Polymer on quartz waveguide sensing platform for enhanced evanescent fluorescence spectroscopy," IEEE Photon. J. **10**, 3901515 (2018).
14. M. Almokhtar, M. Fujiwara, H. Takashima, and S. Takeuchi, "Numerical simulations of nanodiamond nitrogen-vacancy centers coupled with tapered optical fibers as hybrid quantum nanophotonic devices," Opt. Express **22**, 20045 (2014).

15. A. H. J. Yang, S. D. Moore, B. S. Schmidt, M. Klug, M. Lipson, and D. Erickson, "Optical manipulation of nanoparticles and biomolecules in sub-wavelength slot waveguides," Nature **457**, 71 (2009).
16. V. R. Almeida, Q. Xu, C. A. Barrios, and M. Lipson, "Guiding and confining light in void nanostructure," Opt. Lett. **29**, 11 (2004).
17. M. Davanço and K. Srinivasan, "Hybrid gap modes induced by fiber taper waveguides: application in spectroscopy of single solid-state emitters deposited on thin films," Opt. Express **18**, 10995 (2010).
18. D. Yang, X. Chen, and X. Zhang, "Ultrasmall in-plane demultiplexer enabled by an arrayed one-dimensional photonic crystal nanobeam cavity," Opt. Eng. **57**, 107103 (2018).
19. M. A. Butt, C. Tyszkiewicz, P. Karasiński, M. Zięba, D. Hlushchenko, T. Baraniecki, A. Kaźmierczak, R. Piramidowicz, M. Guzik, and A. Bachmatiuk, "Development of a low-cost silica-titania optical platform for integrated photonics applications," Opt. Express **30**, 23678 (2022).
20. M. Rigler, T. Troha, W. Guo, R. Kirste, I. Bryan, R. Collazo, Z. Sitar, and M. Zgonik, "Second-harmonic generation of blue light in GaN waveguides," Appl. Sci. **8**, 1218 (2018).
21. A. Stolz, E. Cho, E. Dogheche, Y. Androussi, D. Troadec, D. Pavlidis, and D. Decoster, "Optical waveguide loss minimized into gallium nitride based structures grown by metal organic vapor phase epitaxy," Appl. Phys. Lett. **98**, 161903 (2011).
22. M. Davanço and K. Srinivasan, "Fiber-coupled semiconductor waveguides as an efficient optical interface to a single quantum dipole," Opt. Lett. **34**, 16 (2009).
23. F. A. Inam, T. Gaebel, C. Bradac, L. Stewart, M. J. Withford, J. M. Dawes, J. R. Rabeau, and M. J. Steel, "Modification of spontaneous emission from nanodiamond colour centres on a structured surface," New J. Phys. **13**, 073012 (2011).